ELSEVIER

Journal of Nuclear Materials 283–287 (2000) 628–632

journal of nuclear materials

www.elsevier.nl/locate/jnucmat

Biaxial thermal creep of V–4Cr–4Ti at 700°C and 800°C

R.J. Kurtz *, M.L. Hamilton

Pacific Northwest National Laboratory, P.O. Box 999, Richland, WA 99352, USA

Abstract

A study of the thermal creep properties of V–4Cr–4Ti were performed using pressurized tube specimens. Creep tubes nominally 4.57 mm OD by 0.25 mm wall thickness were pressurized with high-purity helium gas to mid-wall effective stresses below the uniaxial yield strength. Specimens were heated to 700°C and 800°C in an ultra-high vacuum furnace and periodically removed to measure the change in OD with a high-precision laser profilometer. The secondary creep rate was found to be power-law dependent on the applied stress with a stress exponent of 3.7 at 700°C and 2.7 at 800°C. The average activation energy for creep of V–4Cr–4Ti was 299 kJ/mol, which is quite close to the activation energy for self-diffusion in pure vanadium in this temperature regime. The predominant mechanism of creep deformation for the conditions employed in this study is most likely climb-assisted dislocation motion.

1. Introduction

Vanadium-base alloys are attractive candidate materials for fusion first-wall/blanket structural materials, in part, because of their potentially high service temperatures. The maximum operating temperature limit for vanadium alloys in fusion power system design studies are typically assumed to be about 700°C [1]. Alternately, it was recently suggested that vanadium alloys might be capable of operating at temperatures up to 750°C [2]. The maximum operating temperature will be governed by helium embrittlement, compatibility with the fusion environment and creep resistance (both thermal and irradiation). Information on the creep properties of vanadium and vanadium alloys is limited since only a few studies have been performed [3–8]. Within the existing database there are uncertainties which may have influenced the results such as the starting interstitial impurity content of test specimens and vacuum quality. Because of this paucity of data, it is a priority for the US Advanced Materials program to characterize the creep and creep-rupture properties of the reference vanadium alloy V–4Cr–4Ti.

A study of the biaxial thermal creep properties of V–4Cr–4Ti is being performed using pressurized tube specimens. The specimen geometry, stress levels and test temperatures are designed to complement ongoing efforts to characterize the irradiation creep performance of the same alloy [9–12]. The current study is a companion to another research effort underway at Argonne National Laboratory (ANL) [13] to evaluate the uniaxial creep behavior of V–Cr–Ti alloys as a function of temperature in the range 650–800°C and at applied stress levels between 75 and 380 MPa. The objective of the ANL effort is to characterize the influence of interstitial and substitutional solutes on creep performance.

2. Experimental procedure

Sections of V–4Cr–4Ti tubing with a nominal 4.572 mm OD, 0.254 mm wall thickness and ~45% cold work level were obtained from ANL for fabricating creep specimens. Details of the tubing fabrication have been reported previously [11]. Specimen blanks 25.4 mm long were cut from the tubing and measurements of the ID and OD were performed at two axial locations ($x/l = 1/3$ and 2/3) and at 45° azimuthal intervals prior to cleaning. Prior to welding, specimen blanks and end-caps were degreased and pickled for 3 min in a solution of 40 ml HF, 40 ml HNO_3, 120 ml lactic acid and 100 ml distilled

* Corresponding author. Tel.: +1-509 373 7515; fax: +1-509 376 0418.

E-mail address: rj.kurtz@pnl.gov (R.J. Kurtz).

0022-3115/00/$ - see front matter
PII: S0022-3115(00)00274-9

water to remove surface oxides. After pickling, all parts were rinsed thoroughly with distilled water, acetone, and ethanol to remove any residual chemicals. Following cleaning, the specimen thickness was measured using a metallurgical microscope at eight equally spaced azimuthal locations around each tube end. Five TEM disks punched from pure titanium foil were inserted into each specimen and end-caps were electron-beam welded to the tubes. Following end-cap welding, the specimens were loosely wrapped with titanium foil and annealed in a vacuum ($\leqslant 10^{-7}$ Torr) at 1000°C for 1 h. This heat treatment produced a microstructure with an average grain size of 21 μm. After heat treatment, specimen ODs were re-measured using a laser profilometer. The sensitivity of the laser profilometer is $\pm 5 \times 10^{-4}$ mm which translates to a strain measurement sensitivity of about ±0.01%. The diameter measurements were made at five axial locations (x/l of 0.1, 0.3, 0.5, 0.7 and 0.9). Specimens were then filled with 99.999% purity helium gas to the desired pressure and sealed by laser welding. Fill pressures were determined with a computer code that accounted for the thermal expansion of the tubing and compressibility of the helium fill gas at the test temperature of interest. The specimen OD was again measured using the laser profilometer to determine the elastic diametral displacements for each tube. Prior to insertion into the vacuum furnace, each specimen was loosely wrapped with titanium foil to provide additional protection against oxygen pickup during the experiment. Initially, tube diameters were measured weekly until it was apparent that longer intervals could be tolerated. Two tube sections without end-caps were also included with the pressurized specimens at each test temperature to enable periodic assays for oxygen pickup.

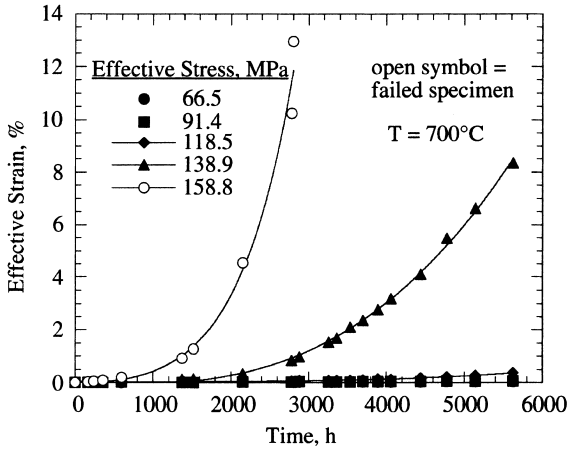

Fig. 1. Time dependence of effective mid-wall creep strain at 700°C for unirradiated V–4Cr–4Ti.

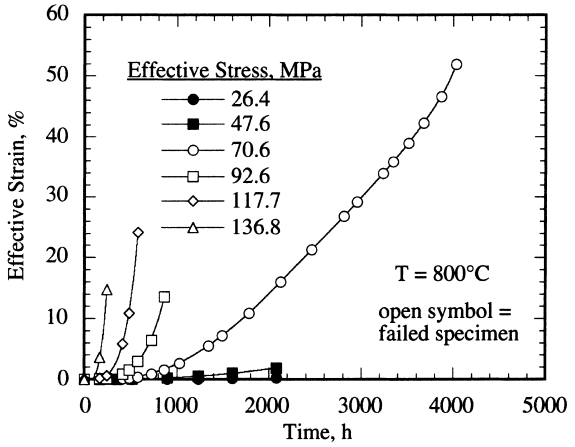

Fig. 2. Time dependence of effective mid-wall creep strain at 800°C for unirradiated V–4Cr–4Ti.

3. Results

Tube diameters were measured as a function of time using the same equipment and procedures as before test. Figs. 1 and 2 show the time dependence of the effective mid-wall creep strains for the 700°C and 800°C test temperatures, respectively. To preclude end effects, only the middle three measurements along the length of the tube were used to compute the average diametral strain. For ruptured specimens, the creep strain is based on the diameter measurement taken nearest the failure location. Creep strains were calculated from the total measured strain minus the elastic contribution. Conversion from outer diameter strain to mid-wall hoop strain was done using the expression derived by Gilbert and Blackburn [14]. It should be noted that the conversion factor is not a constant, but decreases with increasing strain. The Gilbert and Blackburn expression was evaluated numerically to give values of the conversion factor up to diametral strains of 0.6. Mid-wall hoop strains were then converted to effective strains by

$$\varepsilon_e = \frac{2}{\sqrt{3}}\varepsilon_h, \tag{1}$$

where ε_e is the effective mid-wall creep strain and ε_h is the mid-wall hoop strain. Effective mid-wall stresses were calculated from the von Mises distortion energy criterion. The principal stresses inserted into the von Mises equation were the appropriate expressions for stress in a thick-wall, closed end cylinder.

Interesting features of the strain–time curves are that primary creep was not observed and the secondary creep regime was very short. Their shapes are suggestive of predominant tertiary creep from a very early stage in the test. Given that strain measurements are periodic, it is

not surprising that primary creep is not seen since this deformation transient is expected to be of short duration. It is more surprising that the secondary creep regime is apparently also of very short duration. This behavior may be due to the presence of shallow longitudinal scratches or defects found on the tube ID. Results of microstructural examinations of several ruptured specimens and as-received tubes indicate that these defects are common and are probably caused by the tube fabrication technique [15]. Further work is needed to fully assess the significance of these defects on the biaxial creep properties of V–4Cr–4Ti. The reader should also note the relatively high rupture strain of the 800°C specimen tested at 70.6 MPa compared to the rupture strains of the 800°C specimens tested at high stresses. This result is contrary to expectation since creep ductility generally decreases with decreasing stress. This difference may be due to the presence of fabrication defects decreasing the rupture strain of the high-stress specimens, or to strengthening of the 70.6 MPa specimen due to gradual oxygen pickup during the course of the test, or a combination of both. As noted below, some oxygen was picked up during our tests, but it is difficult to quantify its effect on creep ductility. Secondary creep rates were determined by fitting the strain–time data to a straight line for effective strains less than about 0.2%. Very good to excellent curve fits were obtained at these small strain levels. Deviation from linearity was typically found at higher effective strains.

Chemical analyses for pickup of oxygen and nitrogen were performed on two of the unpressurized 800°C tube specimens (Sample IDs: 8-2 and 8-1). These specimens were in the vacuum furnace for 2812 and 5142 h, respectively. The chemical analyses were performed at Siemens Power Corporation in Richland, Washington. The specimens were sectioned into three parts and each section was prepared by etching in 10% HNO_3: 4.8% HF for 30 s to one min followed by deionized water and acetone rinses with air drying. A LECO TC436 nitrogen oxygen determinator was used for the analyses. The method uses inert gas fusion of the sample in a graphite crucible with a nickel flux. Nitrogen is measured by thermal conductivity, and oxygen is measured as carbon dioxide by an infrared detector. Several control standards were analyzed along with the test samples. The average oxygen and nitrogen levels are 733 and 59.8 wppm after 2812 h, and 1044 and 89.5 wppm after 5142 h. These levels may be compared with the as-received values of 699 wppm O and 75 wppm N. The data indicate that a relatively modest increase in oxygen level was experienced during the course of the exposure at 800°C. Any oxygen pickup should only affect the time-to-rupture and not the secondary creep rate since the secondary creep regime was of such short duration in our tests.

4. Discussion

The stress dependence of the effective secondary creep rate is presented in Fig. 3 along with uniaxial data obtained by Chung et al. [8] at 600°C and higher stresses. All of the data in Fig. 3 were fitted to

$$\dot{\varepsilon}_e = A\sigma_e^n, \tag{2}$$

where $\dot{\varepsilon}_e$ is the effective secondary creep rate, σ_e the effective stress and A and n are constants. Note the stress exponent, n, is 9.9 for the 600°C data gathered at stress levels greater than 300 MPa. Stresses above 300 MPa are beyond the 600°C yield strength for V–4Cr–4Ti, so it is reasonable to expect that the stress dependence of the secondary creep rate may differ from data taken at lower stresses. For 700°C and 800°C, data generated at stresses less than 160 MPa (below yield), n is between 2.7 and 3.7. This difference in stress exponent is not due to biaxial versus uniaxial specimen geometries, but is characteristic of creep in vanadium and vanadium alloys [3–8]. Values of $n \sim 3$ suggest that dislocation creep is the predominant deformation mechanism for the thermal and stress conditions employed here [16]. Microstructural studies of several ruptured creep specimens support this conclusion [15].

The activation energy for creep in V–4Cr–4Ti was estimated at effective stress levels of approximately 70, 90 and 120 MPa. Eq. (3) was used to compute the activation energy, Q, as

$$Q = \frac{R \ln(\dot{\varepsilon}_1/\dot{\varepsilon}_2)}{(1/T_1) - (1/T_2)}, \tag{3}$$

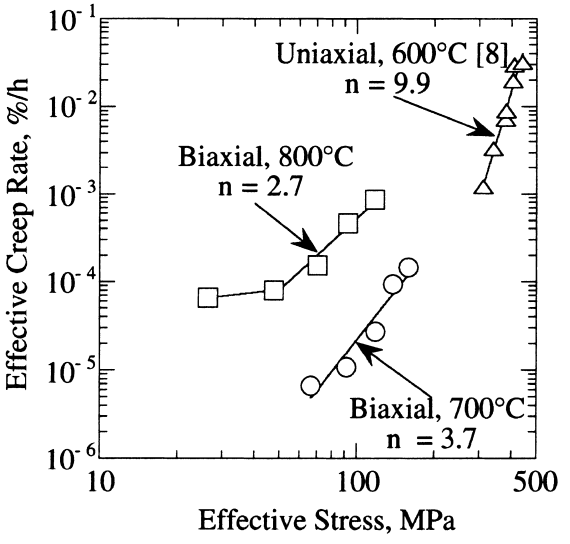

Fig. 3. Stress dependence of the minimum creep rate of unirradiated V–4Cr–4Ti between 600 and 800°C.

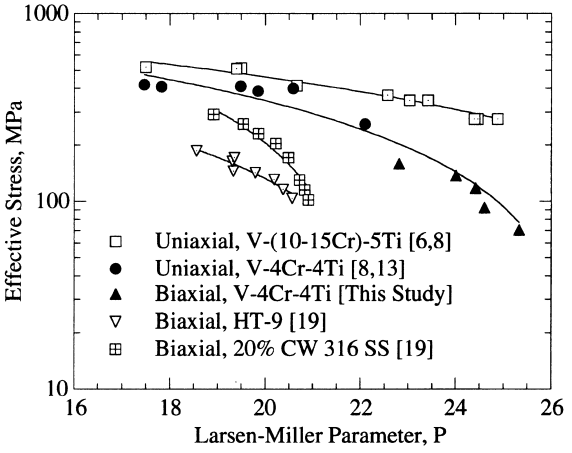

Fig. 4. LMP correlation for creep-rupture of unirradiated V–4Cr–4Ti.

where R is the universal gas constant, and $\dot{\varepsilon}_1$ and $\dot{\varepsilon}_2$ are the effective creep rates at temperatures T_1 and T_2. Activation energies ranging from 272 to 326 kJ/mol were obtained with an average value of 299 kJ/mol. The activation energies did not vary inversely with stress as has been observed for pure vanadium [3]. These values are somewhat greater than the activation energy for self-diffusion in pure vanadium, which is about 270 kJ/mol in the 700–800°C temperature range [18]. This result lends additional support to the observation that the predominant creep mechanism in V–4Cr–4Ti at the temperatures and stresses investigated in this study are climb-assisted glide of dislocations. It also suggests that solute-drag may limit the rate at which dislocations can climb past obstacles in the microstructure leading to a higher activation energy for creep. A recent study of the high-temperature deformation behavior of V–4Cr–4Ti shows that dynamic strain aging occurs in this material at temperatures up to 750°C [17]. This indicates that solutes are mobile at the test temperatures investigated in this study and could impede dislocation climb.

A comparison of the creep-rupture behavior of specimens tested here to data gathered on V–Cr–Ti alloys [6,8,11,13] and other fusion relevant materials [19] is presented in Fig. 4. Both uniaxial and biaxial data are plotted in Fig. 4. The data sets are correlated using the Larsen–Miller parameter (LMP), that is,

$$P = \frac{T(\log t_r + 20)}{1000}, \tag{4}$$

where T is the test temperature in K and t_r is the time-to-rupture in hours. Since failure strains for the vanadium alloys were generally large, a good correlation between uniaxial (constant load tests) and biaxial (constant stress tests) data might not be expected, but this is obviously not the case here. The trend line for V–4Cr–4Ti is quite reasonable, but the data are too sparse to firmly establish an LMP creep-rupture correlation for this alloy. Comparison with V–(10–15)Cr–5Ti data [6,11] indicates that an additional 6–9% Cr improves the creep-rupture properties of this alloy system considerably. Comparing the performance of V–4Cr–4Ti with HT-9 [19] and 20% cold-worked 316 stainless steel [19] shows that V–Cr–Ti alloys exhibit much better creep-rupture resistance and therefore could tolerate higher average wall temperatures.

5. Conclusions

A study of the thermal creep properties of V–4Cr–4Ti was performed using pressurized tube specimens. The secondary creep rate was found to be power-law dependent on the applied stress with a stress exponent of 3.7 at 700°C and 2.7 at 800°C. The average activation energy for creep of V–4Cr–4Ti was 299 kJ/mol, which is quite close to the activation energy for self-diffusion in pure vanadium in this temperature regime. The predominant mechanism of creep deformation for the conditions employed in this study is most likely climb-assisted dislocation motion. Creep-rupture data from uniaxial and biaxial tests of V–4Cr–4Ti specimen yields a reasonable LMP correlation. On this basis the creep-rupture properties of V–4Cr–4Ti were shown to be slightly worse than V–(10–15)Cr–5Ti and significantly better than other candidate fusion structural materials such as HT-9 and 20% cold-worked 316 stainless steel.

Acknowledgements

Work supported by the Office of Fusion Energy Sciences, US Department of Energy under Contract DE-AC06-76RLO 1830. We would like to thank Dr Hanchung Tsai of ANL for supplying the V–4Cr–4Ti tubing and a radiography standard. We also appreciate the substantial contributions of Lee K. Fetrow and Ruby M. Ermi in performing the experiments described in this paper.

References

[1] H. Matsui et al., Fusion Technol. 30 (1996) 1293.
[2] D.L. Smith, M.C. Billone, S. Majumdar, R.F. Mattas, D.-K. Sze, J. Nucl. Mater. 258–263 (1998) 65.
[3] K.R. Wheeler, E.R. Gilbert, F.L. Yaggee, S.A. Duran, Acta Metall. 19 (1971) 21.
[4] M. Shirra, KfK Report 2440, Kernforschungszentrum Karlsruhe, 1989.
[5] H. Boehm, M. Schirra, J. Less-Common Met. 12 (1967) 280.

[6] R.E. Gold, R. Bajaj, J. Nucl. Mater. 122&123 (1984) 759.
[7] T. Kainuma, N. Iwao, T. Suzuki, R. Watanabe, J. Less-Common Met. 86 (1982) 263.
[8] H.M. Chung, B.A. Loomis, D.L. Smith, J. Nucl. Mater. 212–215 (1994) 772.
[9] J.M. Vitek, D.N. Braski, J.A. Horak, J. Nucl. Mater. 141–143 (1986) 982.
[10] V.M. Troyanov et al., J. Nucl. Mater. 233–237 (1996) 381.
[11] H. Tsai, M.C. Billone, R.V. Strain, D.L. Smith, H. Matsui, J. Nucl. Mater. 258–263 (1998) 1471.
[12] H. Tsai, R.V. Strain, M.C. Billone, T.S. Bray, D.L. Smith, in: Fusion Materials: Semiannual Progress Report for Period Ending June 30, 1999, DOE/ER-0313/26, p. 36.
[13] K. Natesan, W.K. Soppet, D.L. Rink, in: Fusion Materials: Semiannual Progress Report for Period Ending June 30, 1999, DOE/ER-0313/26, p. 20.
[14] E.R. Gilbert, L.D. Blackburn, J. Eng. Mater. Technol., ASME Trans. (1977) 168.
[15] D.S. Gelles, M.L. Hamilton, R.J. Kurtz, in: Fusion Materials: Semiannual Progress Report for Period Ending June 30, 1999, DOE/ER-0313/26, p. 11.
[16] G.E. Dieter, Mechanical Metallurgy, McGraw-Hill, New York, 1986, p. 447.
[17] A.F. Rowcliffe, D.T. Hoelzer, S.J. Zinkle, in: Fusion Materials: Semiannual Progress Report for Period Ending June 30, 1999, DOE/ER-0313/26, p. 25.
[18] D.L. Harrod, R.E. Gold, Int. Met. Rev. 4 (1980) 163.
[19] B.A. Chin, in: Proceedings of Topical Conference on Ferritic Alloys for use in Nuclear Energy Technologies, 1983, p. 593.